# Relaxation processes of photoexcited carriers in GaAs/AlAs multiple quantum well structures grown by molecular beam epitaxy at low temperatures

M. C. Rath, T. Araya, S. Kumazaki, K. Yoshihara, and N. Otsuka[a)]
*School of Materials Science, Japan Advanced Institute of Science and Technology, Asahidai 1-1, Tatsunokuchi, Ishikawa 923-1292, Japan*

(Received 24 March 2003; accepted 6 June 2003)

The relaxation processes of photoexcited carriers in GaAs/AlAs multiple quantum well structures grown at low temperatures by molecular beam epitaxy were studied by a tunable single-beam femtosecond pump–probe method. Concentrations of singularly ionized antisite arsenic ions, $As_{Ga}^{+}$, in the quantum wells, which were considered as traps of photoexcited carriers, were estimated from flux conditions and substrate temperatures in the growth. Transient transmittivity of the structures were measured by varying the pump–probe photon energy. The trapping rate of photoexcited carriers, which corresponded to the reciprocal of the carrier lifetime, was derived from the relaxation profile at the pump–probe photon energy close to the exciton resonant excitation energy for each structure. The trapping rate was found to increase linearly with $As_{Ga}^{+}$ in a lower concentration range and superlinearly in a higher concentration range. Photoluminescence and absorption spectra were observed at room temperature and their correlation to the carrier lifetimes were investigated. © *2003 American Institute of Physics.* [DOI: 10.1063/1.1595142]

## I. INTRODUCTION

A GaAs layer grown by molecular beam epitaxy (MBE) at a low temperature (LT-GaAs) has been considered as an important material for ultrafast optoelectronic applications such as ultrafast detectors, pulse generators and photomixers.[1] Among a number of properties of LT-GaAs, a very short lifetime of photoexcited carriers is most important. Relaxation processes of photoexcited carriers in LT-GaAs and $Al_xGa_{1-x}As$/GaAs multiple quantum well structures grown by MBE at low temperatures multiple quantum well (LT-MQW), hence, have been intensively studied in the past decade.

In LT-GaAs and LT-MQW photoexcited carriers are trapped by excess As point defects or As clusters, the latter being formed by post-growth annealing.[2] There have been many studies which analyzed relaxation processes in LT-GaAs and LT-MQW by utilizing models of trapping processes by these excess As point defects and As clusters, but only a few studies have investigated correlations between relaxation processes and experimentally characterized structures related to excess As. Loukakos *et al.* have recently investigated the dependence of the carrier lifetimes on spacings and sizes of As clusters, which were characterized by using transmission electron microscopy (TEM).[3] They found that the relationship predicted by Ruda and Shik was applicable.[4] As for excess As point defects, a number of studies have analyzed relaxation processes on the basis of rate equations,[5–8] but no study has reported a dependence of the carrier lifetime on experimentally determined concentrations of excess As point defects in LT-GaAs or LT-MQW. Only the dependence of the carrier lifetime on the growth temperature[9–15] or the flux conditions[16] has been investigated, and hence, its dependence on the excess As concentrations has been only qualitatively discussed to date.

In the present article, we report a study on the relaxation processes of photoexcited carriers in LT-MQW structures. GaAs/AlGaAs MQW structures grown at the normal substrate temperature, that is, at about 600 °C, are known to exhibit large optical nonlinearity at room temperature due to the optically induced change in the exciton resonant excitation.[17] A recent study by Okuno *et al.*[13] has shown that LT-MQW structures also exhibit large optical nonlinearity at room temperature and, in addition, have very fast relaxation. In the present study, from the As/Ga flux ratios and the growth temperatures, concentrations of singularly ionized antisite As, $As_{Ga}^{+}$, which is considered as the main trap of photoexcited carriers in LT-GaAs,[10] were determined by utilizing a relation derived in earlier growth studies.[18,19] Carrier lifetimes were measured by utilizing pump-probe experiments. The present study, therefore, has revealed a quantitative dependence of the relaxation time of photoexcited carriers on the trap density in as-grown LT-MQW. The results show that the trapping rate, which corresponds to the reciprocal of the carrier lifetime, increases linearly with the concentration of $As_{Ga}^{+}$ in a lower concentration range but superlinearly in a higher concentration range. This result differs from the relation based on the Shockley-Read-Hall (SRH) theory for the recombination process of photoexcited carriers,[20,21] which has been used in describing the dependence of the carrier lifetime on the trap density in LT-GaAs.[9,15] Because of the MQW structures, photoluminescence emission and exciton absorption spectra were observed

a)Author to whom correspondence should be addressed; electronic mail: ootsuka@jaist.ac.jp

 

at room temperature from the samples with relatively low excess As concentrations. Their correlations with measured carrier lifetimes are discussed in the present article.

## II. MBE GROWTH AND STRUCTURE CHARACTERIZATION

Six AlAs/GaAs MQW samples were grown on epi-ready (100) GaAs substrates by utilizing a conventional MBE system. After the growth of a 150-nm-thick GaAs buffer layer and an 800-nm-thick etch-stop AlAs layer at 580 °C, a MQW structure with 50 periods of a 7.5-nm-thick GaAs layer and a 3.5-nm-thick AlAs layer was grown without rotation of the substrate. As explained in detail later, the growth was carried out without substrate rotation in order to obtain very low excess As concentrations in a highly controlled manner. However, this resulted in nonuniform fluxes of Ga and Al over the growth surface and, hence, slightly different well and barrier thicknesses among different positions of a MQW sample. One MQW sample named HT, was grown at 580 °C with ion gauge readings of the Ga, Al, and As fluxes being $5.2\times10^{-7}$, $8.8\times10^{-8}$, and $2.6\times10^{-5}$ Torr, respectively. Two LT-MQW samples, LT1 and LT2, were grown at 300 °C with the above Ga and Al fluxes and the As fluxes being nearly $6.2\times10^{-6}$ Torr with a slight difference between the two samples. According to our earlier study,[22] this flux condition is known to give rise to nearly stoichiometric LT-GaAs samples at a low substrate temperature. Other two MQW samples, LT3 and LT4, were grown at 300 °C with the same Ga and Al fluxes as LT1 and LT2 samples but with the As flux being $9.4\times10^{-6}$ and $1.2\times10^{-5}$ Torr, respectively. The last MQW sample, LT5, was grown at 270 °C with the As flux similar to that of LT4 and with the above Ga and Al fluxes.

Concentrations of antisite As in all LT-MQW samples were estimated by using the As/Ga flux ratio and growth temperature. In an earlier study[18] we found that for a given growth temperature the concentration of $As_{Ga}$, $[As_{Ga}]$, in a LT-GaAs layer is expressed by

$$[As_{Ga}] = \frac{J_{As}/J_{Ga} - 1}{J_{As}/J_{Ga}} [As_{Ga}]_{sat}, \quad (1)$$

where $J_{As}$ and $J_{Ga}$ are atomic fluxes representing numbers of atoms arriving at a unit surface area for a unit time of As and Ga, respectively, and $[As_{Ga}]_{sat}$ is a saturated concentration of $As_{Ga}$ at a high As/Ga flux ratio. The saturated concentration $[As_{Ga}]_{sat}$ at the growth temperature of 300 and 270 °C are $2.4\times10^{19}$ and $5.2\times10^{19}$ $cm^{-3}$, respectively.[18]

Because of no rotation of a substrate during the growth, the As/Ga flux ratio slightly varies from one end of the substrate surface to the other end. The position dependence of flux ratios $J_{As}/J_{Ga}$ in LT1 and LT2 samples were estimated in the following way. The gradient of $J_{As}/J_{Ga}$ along the substrate surface is 0.008/mm. The surface of a LT-GaAs layer, on the other hand, becomes nonspecular when $J_{As}/J_{Ga}$ is less than unity.[22] The value of $J_{As}/J_{Ga}$ at a given position of a nearly stoichiometric LT-MQW sample, therefore, can be determined by its location with respect to the boundary between the specular and non-specular surfaces. The gradient of $J_{As}/J_{Ga}$ along the substrate surface was also estimated from a shift of this boundary between the two samples grown with slightly different values of the ion gauge reading of As fluxes. Concentrations $[As_{Ga}]$ of these positions were then derived from the values of $J_{As}/J_{Ga}$ by using Eq. (1).

TABLE I. Atomic flux ratios in the MBE growth and concentrations of $As_{Ga}$ and $As_{Ga}^{+}$ of the LT-MQW samples.

| Sample | $J_{As}/J_{Ga}$ | $[As_{Ga}]$ ($cm^{-3}$) | $[As_{Ga}^{+}]$ ($cm^{-3}$) |
|---|---|---|---|
| LT1 | 1.07 | $1.48\times10^{18}$ | $7.4\times10^{16}$ |
| LT2 | 1.12 | $2.52\times10^{18}$ | $1.26\times10^{17}$ |
| LT3 | 1.53 | $8.31\times10^{18}$ | $4.15\times10^{17}$ |
| LT4 | 1.96 | $1.17\times10^{19}$ | $5.85\times10^{17}$ |
| LT5 | 2.08 | $3.08\times10^{19}$ | $1.54\times10^{18}$ |

The values of $J_{As}/J_{Ga}$ of the LT3, LT4, and LT5 samples were determined simply from its ion gauge reading of the As flux with respect to the ion gauge reading of nearly stoichiometric LT-MQW samples, because $[As_{Ga}]$ changes slowly with the As/Ga flux ratio in the high flux ratio range.[18] Concentrations of excess As in AlAs layers in LT-MQW samples were not estimated because no quantitative data are available for the dependence of the concentration on the growth conditions. The excess As concentration in AlAs layers, however, are considered to change with the growth condition in a similar manner to those in GaAs layers.

Luysberg *et al.* have reported the concentrations of neutral $As_{Ga}$ and $As_{Ga}^{+}$ in a number of LT-GaAs samples.[19] They found that the ratio of the concentration of $As_{Ga}^{+}$ to that of neutral $As_{Ga}$ was nearly constant and approximately 5%. The concentrations of $As_{Ga}$ and $As_{Ga}^{+}$ of the LT-MQW samples, the latter of which is assumed to be 5% of the former, are listed in Table I. On the basis of the derivations of Eq. (1) from the experimental results[18] and the variation of the ratio of reported $[As_{Ga}^{+}]$ to $[As_{Ga}]$,[19] the deviation of $[As_{Ga}^{+}]$ listed in Table I from the actual concentrations in the samples is considered to be less than 10%.

The structure of the LT-MQW samples was examined by using a cross-sectional TEM. There are extended defects such as stacking faults and dislocations in the region where $J_{As}/J_{Ga}$ ratio is very close to unity, but all MQW regions that were used for optical measurements in the present study were found to be free from any extended defects and As clusters as seen from a TEM image of the LT4 sample in Fig. 1. The TEM image shows a cross-sectional view of a defect-free MQW structure from its interface with the GaAs buffer to the free surface. Dark bands in the right-hand side of the image are bending contours of a thin TEM sample. For the pump–probe and optical absorption measurements, a MQW sample was mounted on a glass plate, and the GaAs substrate and buffer layer were removed by the selective chemical etching procedure.[23]

## III. OPTICAL ABSORPTION AND PHOTOLUMINESCENCE MEASUREMENTS

The room temperature absorption spectra of high temperature (HT) and five LT-MQW samples are shown in Fig. 2. All MQW samples except LT5 exhibit two distinct exciton

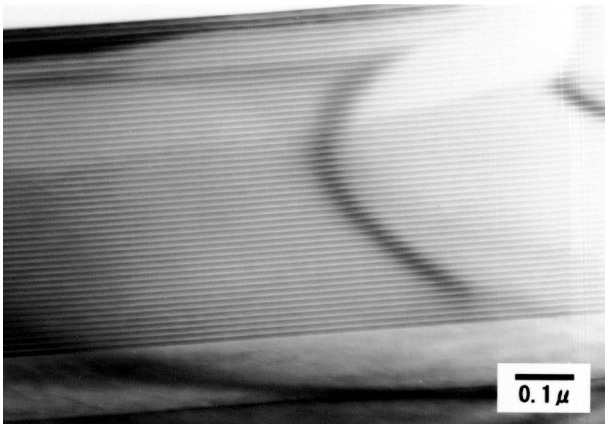


FIG. 1. Cross-sectional bright field TEM image of a low-temperature grown MQW GaAs/AlAs (LT4) sample. The dark bands on the right-hand side of the image are bending contours of a thin cross-sectional TEM sample.

absorption peaks. The two exciton absorption peaks gradually broaden with the excess As concentrations. The higher energy peak corresponds to the light hole (lh) exciton absorption peak, and the lower energy peak to the heavy hole (hh) exciton absorption peak. The two peaks are separated by

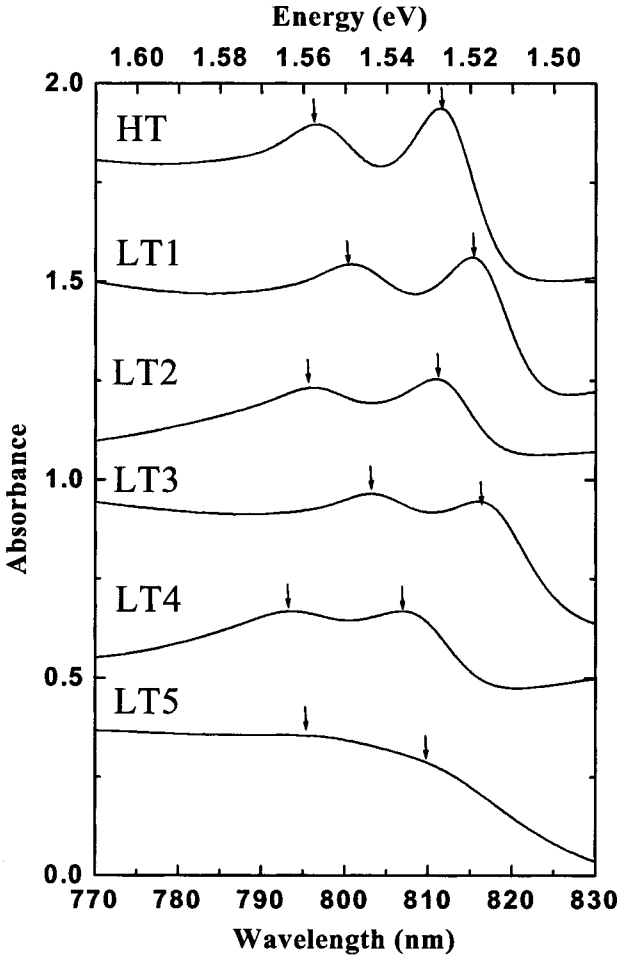


FIG. 2. Absorption spectra of normal substrate temperature grown MQW sample, HT, and five LT-MQW samples at room temperature. Position of the arrows indicates lh exciton absorption peak and hh exciton absorption peak in all case.

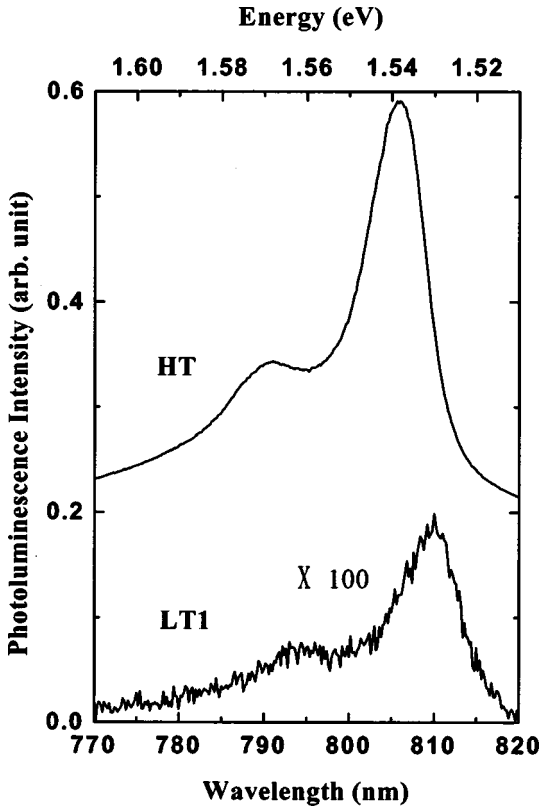


FIG. 3. Photoluminescence spectra of a normal substrate temperature grown MQW sample, HT, and a near-stoichiometric LT-MQW sample, LT1, at room temperature.

about 15 nm corresponding to an energy difference of about 30 meV. The differences of the exciton absorption peak positions among the samples are ascribed to the differences in their GaAs well widths and AlAs barrier widths which are explained in the previous section.

Photoluminescence measurements were carried out at 4.5 K and at room temperature by using the 488 nm output of an argon ion laser as an excitation source and an InGaAs detector. Photoluminescence peaks were observed from the HT sample and two nearly stoichiometric LT-MQW samples, LT1 and LT2, both at 4.5 K and room temperature, but no detectable photoluminescence peaks were observed from the other three samples, LT3, LT4, and LT5 at either temperature. The photoluminescence peaks observed from the HT and LT1 samples at room temperature are shown in Fig. 3. The observed photoluminescence (PL) peaks resulted from excitonic transitions in the GaAs well layers. The separation between the two peaks in each sample is about 30 meV which is equal to the separation between the lh and hh exciton absorption peak positions in the absorption spectra. The slight difference between the PL peak positions and excitonic absorption peak positions in each sample is attributed to the differences in their GaAs well widths and AlAs barrier widths at different sample positions used for the PL and absorption measurements. The PL peak intensity of the HT sample is approximately 200 times higher than that of the nearly stoichiometric LT-MQW sample, LT1, at room temperature as seen in Fig. 3. The PL intensity of another nearly stoichiometric LT-MQW sample, LT2, is also of the similar

order of the magnitude lower than that of the HT sample at room temperature.

## IV. PUMP–PROBE TRANSIENT MEASUREMENT

Single wavelength pump-probe experiments were carried out at room temperature by using a mode-locked Ti:sapphire laser (Clark-MXR) pumped by an argon ion laser. The central wavelength of the oscillator output was tuned from 765 nm to 830 nm. The band width (FWHM) of the output beam gradually decreased from 25 nm for the central wavelength at 765–15 nm for the central wavelength at 830 nm. The repetition rate was 100 MHz. The probe power was fixed at 1 mW and the pump power was kept at 7 $\pm 0.5$ mW in order to minimize complex photoexcitation processes at higher pump power. The spot sizes of the pump and probe beams at the sample position were approximately 200 and 100 $\mu$m, respectively. The transmitted probe beam through the sample was incident on a photodiode detector connected to a lock-in amplifier. Pump and probe pulses were perpendicularly polarized and one polarizer was put before the detector for the probe, in order to avoid scattering of the pump beam. Pump and probe beams were chopped at different frequencies by the outer and inner holes of a chopping wheel, respectively, and the transmission change was obtained as the amplitude of the sum frequency modulation using a lock-in amplifier. The instrument response time was determined to be 80 fs in FWHM by an optical Kerr effect cross correlation between the pump and probe pulses.

The pump–probe experiments were carried out at several different central wavelengths with the samples used for the optical absorption. All measurements were carried out under the same data acquisition (the same lock-in-amplifier phase) conditions. The pump–probe wavelengths were tuned with reference to the absorption spectra shown in Fig. 2. The temporal profiles of the differential transmission signal (DTS) at representative wavelengths in the case of LT1, LT4, and LT5 are shown in Fig. 4. The zero time in our analysis was determined to be the earliest optical delay that gives the first signal substantially above the noise level [signal-to-noise $(S/N) \geqslant 3$)] in the case of the pump-probe measurements of the HT sample. Since our instrument response function has an FWHM of about 80 fs, the pump–probe pulses are significantly overlapping each other in the time between 0 and 100 fs. We, therefore, avoid discussions on the DTS between 0 and 100 fs. The DTS at approximately 100 fs is defined as $DTS_0$. It was observed that the $DTS_0$ gradually increased with increasing the wavelengths in the range lower than the excitonic absorption peak position and reached a maximum value near the lh exciton absorption peak position as seen in Figs. 4(a) and 4(b) for LT1 and LT4. After reaching the maximum value, the $DTS_0$ gradually decreased with further increase in the wavelength, and finally negative $DTS_0$ were obtained at the wavelengths longer than the hh exciton absorption peak position as seen in Figs. 4(a) and 4(b). Similar results were obtained for the HT and other two LT-MQW samples, LT2 and LT3, which had clear exciton absorption peaks.

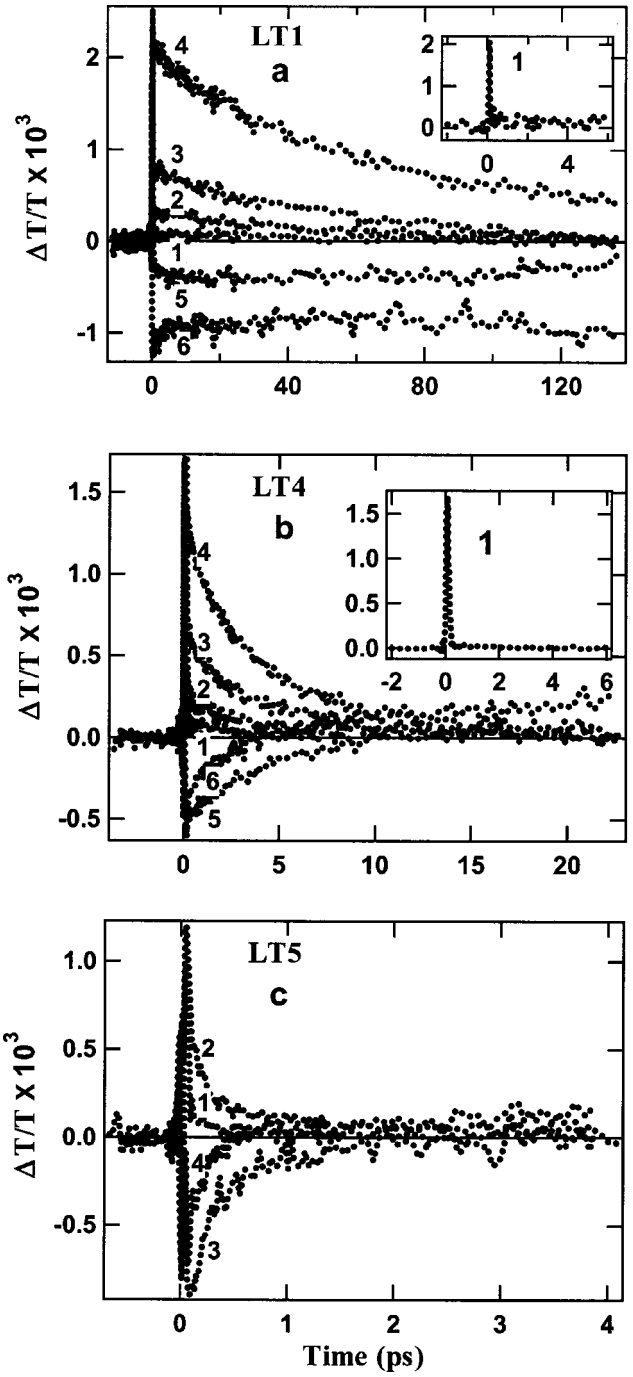


FIG. 4. Differential transmission signal (DTS) profiles obtained at different pump–probe wavelengths for three set of LT-MQW samples, LT1, LT4, and LT5. (a) for LT1, 1, 775 nm; 2, 780 nm; 3, 790 nm; 4, 800 nm; 5, 815 nm; and 6, 820 nm. Inset: expanded DTS profile, 1. (b) for LT4, 1, 765 nm; 2, 770 nm; 3, 780 nm; 4, 790 nm; 5, 805 nm; and 6, 815 nm. Inset: expanded DTS profile, 1. (c) for LT5, 1, 775 nm; 2, 795 nm; 3, 810 nm; and 4, 815 nm; The pump and probe powers were 7 and 1 mW, respectively.

In the case of LT5, where the exciton absorption peaks were not clearly seen, the $DTS_0$ was found to increase gradually from 770 to 795 nm, and then gradually decreased from 795 to 830 nm. In analogy with the case of the other samples, the wavelength of 795 nm, which gave the maximum positive $DTS_0$, was assigned to be the lh exciton absorption peak position. By assuming the same separation between the lh and hh exciton absorption peak positions of

about 15 nm as in the other samples, the hh exciton absorption peak position of LT5 was assigned at 810 nm.

The wavelength dependence of the $DTS_0$ for all the MQW samples in our study are similar to that obtained by Miller *et al.* for GaAs/GaAlAs MQW structures grown at the normal substrate temperature.[24] They used 6 ps pulses with a relatively narrow spectral bandwidth and observed two well-resolved positive peaks in their DTS spectrum corresponding to the lh and hh exciton absorption peak positions and negative DTS values at the positions away from the exciton absorption peaks. The amplitude of the DTS spectral peak near the hh exciton absorption peak position was larger than that near the lh exciton absorption peak position. In the present case, however, we were not able to resolve these two peaks in our $DTS_0$ spectrum mainly because our femtosecond pump–probe spectral band width (about 50 meV) is much broader than that of theirs (about $<5$ meV). The nonlinear transmission of MQW structures grown at the normal substrate temperature was ascribed to the phase space filling effect of photoexcited excitons and to the screening effect by free carriers generated through thermal ionization of photoexcited excitons.[25] The former effect is explained as the loss of the oscillator strength of the resonant excitation because of the occupation of states out of which the excitons are constructed. The latter effect is regarded as the loss of the stability of the excitons due to the screening of the Coulomb interaction of electron–hole pairs by free carriers, which results in the broadening of the exciton resonant absorption peaks. In our case, at the lh exciton absorption peak position, the HT and all the five LT-MQW samples exhibited positive DTS. However, at the hh exciton absorption peak position, except for the HT sample all the five LT-MQW samples exhibited an initial positive DTS, which changed to negative value on a shorter time scale less than about 10 ps.

When the wavelength is shorter by at least 30 nm than the lh exciton peak position, the $DTS_0$ is far smaller than the signal amplitudes earlier than 100 fs, which are instrument-response-limited rise and decay. This can be seen in the DTS profile of LT1 and LT4 at shortest wavelength in the inset of Figs. 4(a) and 4(b). The DTS profiles for all the MQW samples at the wavelength near the lh exciton absorption peak, which show the highest $DTS_0$, are shown in Fig. 5 with their values normalized by $DTS_0$. The normalized DTS profiles of the LT-MQW samples near the lh exciton absorption peak position show a gradual increase in the decay rate from LT1 to LT5. The DTS profiles of these MQW samples at the wavelength near the hh exciton absorption peak are shown in Fig. 6 without any normalization because these profiles are not so simple like those obtained near the lh exciton absorption peak position. The DTS profiles of the LT-MQW samples near the hh exciton absorption peak position, after reaching a maximum negative value, decays towards the zero level. These decay profiles also show a gradual increase in the decay rate from LT1 to LT5 as in the case of the decay profiles near the lh exciton absorption peak position.

It is seen from both Figs. 5 and 6 that in the case of LT3, LT4, and LT5 which contains relatively higher excess $As_{Ga}^{+}$ concentrations, the DTS profiles near both the lh and hh

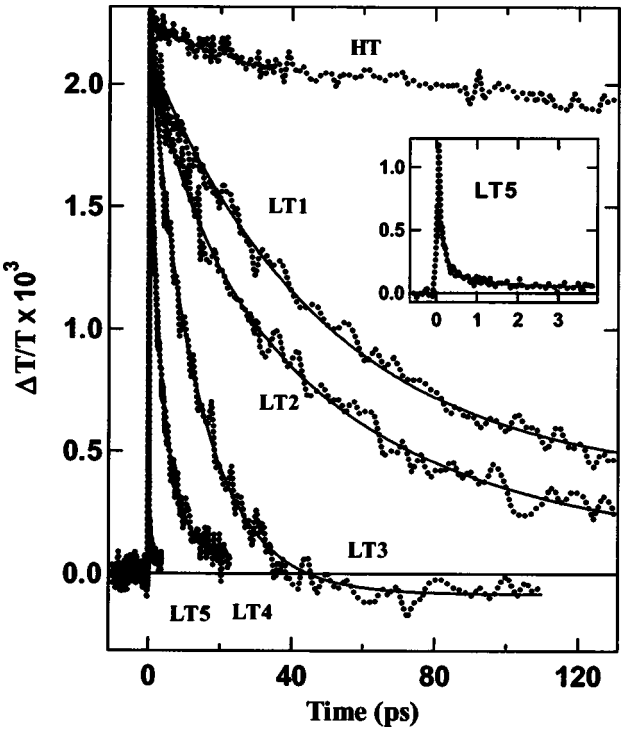


FIG. 5. Normalized DTS profiles of five LT-MQW samples (LT1, LT2, LT3, LT4, and LT5) along with the HT sample for the pump–probe wavelength near the lh exciton absorption peak at room temperature. Inset: DTS profile of LT5 in expanded scales. Dotted and solid lines represent the experimentally obtained DTS profiles and the fitting curves, respectively. The pump and probe powers were 7 and 1 mW, respectively.

exciton absorption peak positions decrease to zero level. The DTS profile of the HT sample near the lh exciton absorption peak position is similar to those reported for the normal temperature grown GaAs/AlAs MQW structures in the literature.[13] The DTS profile of this sample near the lh exciton absorption peak position shows a faster decay compared to that near the hh exciton absorption peak position. The decay profiles of the DTS of the LT-MQW samples near both the lh and hh exciton absorption peak positions were fitted with a biexponential decay function plus a little offset except for LT5. A single exponential decay curve fitting with convolution of the instrument response function was carried out for LT5. The fitting parameters were determined from a number of DTS profiles taken at slightly different sample positions under the same pump–probe conditions. The results obtained from the DTS profiles near the lh and hh exciton absorption peak positions are listed in Tables II and III, respectively. The estimated carrier lifetimes are shown with their errors. The errors associated with the results obtained from DTS profiles obtained near the hh exciton absorption peak position, particularly in the case of LT1, are very large, which is due to the limited time window. In Table II, the weighted average of the two time constants, $\langle\tau\rangle=(a_1\tau_1+a_2\tau_2)/(a_1+a_2)$ was estimated from the data obtained near the lh exciton absorption peak position for the simpler representation of the carrier lifetime. In Table III, the first time constant, $\tau_1$, is related to the decay of DTS from the initial positive values to the negative values. The second time constant, $\tau_2$, is related to the decay of the negative DTS. The

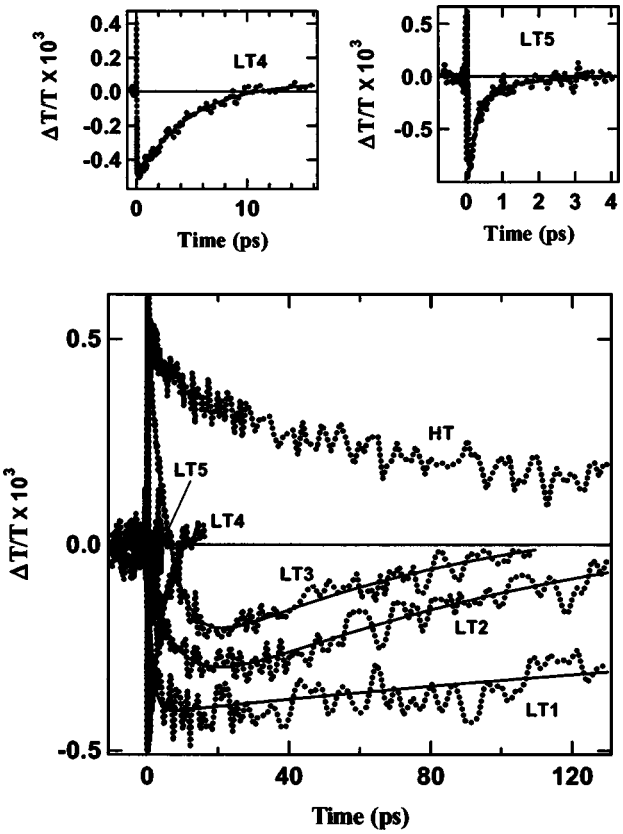


FIG. 6. DTS profiles of five LT-MQW samples (LT1, LT2, LT3, LT4, and LT5) along with the HT sample for the pump–probe wavelength near the hh exciton absorption peak at room temperature. Top: DTS profiles of LT4 and LT5 in expanded scales. Dotted and solid lines represent the experimentally obtained DTS profiles and the fitting curves, respectively. The pump and probe powers were 7 and 1 mW, respectively.

long time constant $\tau_2$ in the case of the hh exciton absorption peak position is much greater than the weighted average time constant $\langle\tau\rangle$ in the case of the lh exciton absorption peak position for the first three LT-MQW samples, LT1, LT2, and LT3. On the other hand, $\tau_2$ is only a little larger than $\langle\tau\rangle$ for the other two LT-MQW samples, LT4 and LT5. The plot of the reciprocal of the weighted average time constant $\langle\tau\rangle$ against $As^+_{Ga}$ concentration is shown in Fig. 7. It shows that the $1/\langle\tau\rangle$ increases linearly with $As^+_{Ga}$ at relatively low concentrations but rapidly increases at higher concentrations, exhibiting a superlinear change. A similar trend was also observed for the plot of $1/\tau_2$ vs $As^+_{Ga}$ concentration where $\tau_2$ is the long time constant listed in Table III.

TABLE II. Carrier lifetimes determined from the DTS profiles obtained with the pump–probe wavelength near the lh exciton absorption peak of the LT-MQW samples at room temperature. Pump and probe powers were 7 and 1 mW, respectively.

| Sample | Amplitude ($a_1$) (%) | $\tau_1$ (ps) | Amplitude ($a_2$) (%) | $\tau_2$ (ps) | $\langle\tau\rangle$ (ps) |
|---|---|---|---|---|---|
| LT1 | 9±2 | 3.9±0.4 | 91±2 | 62.5±6.0 | 57.2±5.5 |
| LT2 | 27±5 | 13.0±1.1 | 73±5 | 55.5±5.2 | 44.0±4.2 |
| LT3 | 35±7 | 9.3±0.8 | 65±7 | 16.0±2.0 | 13.5±1.2 |
| LT4 | 27±5 | 0.6±0.1 | 73±5 | 4.5±0.4 | 3.4±0.3 |
| LT5 | 100 | 0.2±0.04 | | | 0.2±0.04 |

TABLE III. Carrier lifetimes determined from the DTS profiles obtained with the pump–probe wavelength near the hh exciton absorption peak of the LT-MQW samples at room temperature. Pump and probe powers were 7 and 1 mW, respectively.

| Sample | Amplitude ($a_1$) | $\tau_1$ (ps) | Amplitude ($a_2$) | $\tau_2$ (ps) |
|---|---|---|---|---|
| LT1 | 0.4±0.3 | 1.2±1.5 | −0.3±0.2 | 475±200 |
| LT2 | 0.3±0.2 | 9.1±1.0 | −0.5±0.3 | 150±20 |
| LT3 | 0.8±0.3 | 5.9±0.5 | −0.4±0.2 | 80±10 |
| LT4 | 0.2±0.1 | 0.1±0.1 | −0.6±0.2 | 5.1±0.3 |
| LT5 | N.d.[a] | N.d.[a] | −1.2±0.3 | 0.5±0.05 |

[a]N.d.: not detected

## V. DISCUSSION

All the LT-MQW samples examined in the present study exhibit two distinct exciton absorption peaks in their absorption spectra except for the LT5 sample. The photoluminescence and optical absorption measurements suggest that photoexcited carriers in the LT-MQW samples exist in the form of excitons confined in the GaAs quantum wells. TEM observations of these LT-MQW samples showed that the interfaces between the well and barrier layers were smoother in LT4 sample than in the LT1 and LT2 samples. The broadening of the exciton absorption peaks with the excess As concentration, therefore, may be attributed to the presence of excess As point defects in the GaAs well.

The present study has shown that the PL emission from LT-MQW samples becomes weaker as the carrier lifetime is reduced with increasing the excess As concentrations. Under the condition that the pump–probe wavelength is near the lh exciton absorption peak, the carrier lifetime of the LT1 sample is about 57±5 ps, while that of the HT sample is a few nanoseconds as seen from its DTS profile in Fig. 5. The latter is known to be a few tens of nanoseconds for the normal substrate temperature grown GaAs/GaAlAs MQW structures.[26] The shorter carrier lifetime of the HT sample than the reported one is considered to have resulted from a

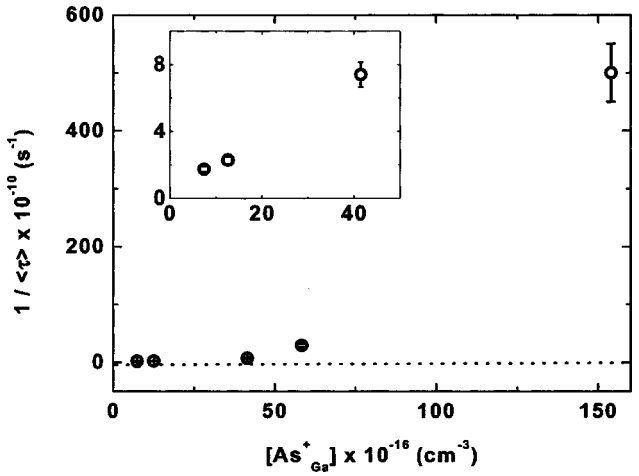


FIG. 7. Plots of the reciprocal of the weighted average time constant $\langle\tau\rangle$ vs $As^+_{Ga}$ concentrations for the pump–probe wavelength near the lh exciton absorption peak position. The inset shows the data points of the three samples, LT1, LT2, and LT3 with relatively low $As^+_{Ga}$ concentrations in a magnified scale.

relatively higher concentration of unintentionally incorporated impurities such as oxygen in our sample. The ratio of PL intensities of these two samples in Fig. 3 is approximately close to the ratio of their carrier lifetimes, which is expected from the fact that excess carrier concentration under a continuous photoexcitation is proportional to the carrier lifetime.

On the other hand, under the condition that the pump–probe wavelength is near the hh exciton absorption peak, the carrier lifetime of the LT1 sample is about $475\pm200$ ps, while that of the HT sample is about 100 ps as seen from its DTS profile in Fig. 6. The latter is much shorter than that obtained when the pump–probe wavelength is near the lh exciton absorption peak position. This may result from the presence of unintentionally incorporated impurities in this HT sample. These impurities did not cause the negative DTS at this pump–probe wavelength unlike excess As atoms but gave rise to the apparent faster decay. The ratio of their PL intensities in Fig. 3 is not close to the ratio of their lifetimes based on the pump–probe results near the hh exciton absorption peak. Based on this comparison, therefore, one can consider that the DTS profiles near the lh exciton absorption peak position can be directly correlated to the population of excess electrons at the bottom of the conduction subband, which is the fluorescent state. The decay time constant in Table II thus represents the carrier trapping process by the $As_{Ga}^{+}$ traps. One possible reason for the difference in the observed DTS profiles for both HT and LT-MQW samples at the lh and hh exciton absorption peak positions could be due to the difference in the spatial size of the lh and hh excitons.

The decay of the negative DTS near the hh exciton absorption peak position is slower than those near the lh exciton absorption peak position, especially in the case of LT1, LT2, and LT3. The relatively long-lived negative DTS near the hh exciton peak may be attributed to the continuation of the excitation of trapped electrons at $As_{Ga}$ defects because it was observed only from the LT-MQW samples.[27] The time constant $\tau_2$ in Table III may thus represent the lifetime of such intermediate non-fluorescent states that are generated before the full recombination of the electron–hole pair. This lifetime seems to be also reduced with the increase of the $As_{Ga}^{+}$ concentration. In the case of LT4 and LT5, $\tau_2$ in Table III is a little larger than the $\langle\tau\rangle$ in Table II, which suggests a short lifetime of the intermediate state in these two samples. The DTS profiles of LT3, LT4, and LT5 at both the lh and hh exciton absorption peaks decrease to zero level, which may suggest a complete recovery to the ground state. The $As_{Ga}^{+}$ concentration dependence of the $\langle\tau\rangle$ in Table II and $\tau_2$ in Table III, hence, suggests that not only the initial trapping of the electrons by the $As_{Ga}^{+}$ defects but also the full recombination process is accelerated by the increase in the $As_{Ga}^{+}$ concentration.

The DTS profiles of the LT-MQW samples at wavelengths shorter than the excitonic absorption peak positions show a significant change in their decay patterns. When the pump–probe photon energy is by about 60 meV higher than the lh exciton absorption peak position, the DTS profiles exhibit instantaneous rise and decay with a very small $DTS_0$ as seen in the inset of Figs. 4(a) and 4(b) for LT1 and LT4, respectively. This indicates that electrons with an excess energy in the quantum well are relaxed down to the bottom of the conduction subband via an intraband scattering process within a time scale known to be less than 200 fs,[28] which is comparable to the instrument response time in our study. Hence, at this pump–probe photon energy, the DTS profiles cannot represent the exact trapping process of carriers by $As_{Ga}^{+}$.

In Fig. 7, the reciprocal of the time constant, $1/\langle\tau\rangle$ increases linearly with $As_{Ga}^{+}$ in the concentration range less than approximately $5\times10^{17}$ cm$^{-3}$ and increases superlinearly in the concentration range greater than $5\times10^{17}$ cm$^{-3}$. The dependence of the carrier lifetime on the trap density is normally described by using the Shockley-Read-Hall (SRH) theory. According the SRH theory, the carrier lifetime, $\tau$, is inversely proportional to the trap density:

$$\tau=\frac{1}{N_d\sigma v_{\mathrm{th}}}, \tag{2}$$

where $N_d$, $\sigma$, and $v_{\mathrm{th}}$ are the trap density, capture cross section of a trap, and thermal velocity of a photoexcited carrier, respectively. This relation has been used in earlier studies on the relaxation process of photoexcited carriers in LT-GaAs.[9,15] Our results in Fig. 7 deviate from the linear relation expected from the SRH theory at the higher $As_{Ga}^{+}$ concentrations.

A linear relation between the carrier lifetime and the trap concentration may be derived as follows without assuming the thermal equilibrium of photoexcited carriers, which is the basis of the SRH theory. First, the decay of photoexcited electrons at the bottom of the subband, which is the main cause of the transient transmissivity, is assumed to be controlled only by the trapping process of the electrons by the $As_{Ga}^{+}$ traps. Second, the trapping processes of photoexcited carriers by $As_{Ga}^{+}$ point defects are assumed to occur independently of one another. With these assumptions, the decay time constant of the excited electrons at the bottom of the subband in a quantum well becomes inversely proportional to $As_{Ga}^{+}$ concentration. Hence, we can replace $\sigma v_{\mathrm{th}}$ in Eq. (2) with a simple proportionality constant, $k$, which can be called the trapping rate constant of photoexcited carriers. The trapping rate constant, $k=1.8\times10^{-7}$ cm$^3$ s$^{-1}$, was obtained from the LT1, LT2, and LT3 samples by using the least-squares method. In neutron-irradiated GaAs, Kruger *et al.* investigated the dependence of the lifetime of photoexcited carriers on the $As_{Ga}^{+}$ concentration, where the concentration of $As_{Ga}^{+}$ was determined by the electron paramagnetic resonance measurements.[29] The $As_{Ga}^{+}$ concentrations in their case are lower than those in our study. As expected from the above explanation, their results exhibit a linear relation between $1/\tau$ and $As_{Ga}^{+}$ concentrations. From their results, the trapping rate constant $k$ is estimated to be $1.5\times10^{-7}$ cm$^3$ s$^{-1}$. This is very close to the value obtained in our study, which implies that the relaxation process of photoexcited carriers in the LT-MQW samples with relatively low $As_{Ga}^{+}$ concentrations is similar to that in the neutron-irradiated GaAs. The significant deviation from the linearity in the relatively high excess $As_{Ga}^{+}$ concentrations range suggests a possibility of a different relaxation process from the trapping of photoexcited carriers, which occurs in the low

$As_{Ga}^{+}$ concentrations. However, clarification of the origin of this superlinearity requires further investigations of the relaxation processes in LT-MQW as well as LT-GaAs.

In summary, the relaxation process of photoexcited carriers in LT-GaAs/AlAs MQW samples has been studied by the combination of time-resolved optical measurements and MBE growth experiments. The trapping rate of photoexcited carriers changes linearly with the experimentally determined $As_{Ga}^{+}$ concentrations in the GaAs well layers in a low concentration range and changes superlinearly in a higher concentration range. The trapping rate constant in the low concentration range, $k=1.8\times10^{-7}\ \mathrm{cm}^3\,\mathrm{s}^{-1}$, is close to that in the case of neutron-irradiated GaAs, which indicates a similar carrier trapping mechanism in the two cases. We have also found that not only the initial trapping of the carriers by the $As_{Ga}^{+}$ traps, but also the full recombination process appears to be accelerated by the increase of these trap concentrations.

[1] J. F. Whitaker, in *Properties of Gallium Arsenide*, 3rd ed., edited by M. R. Brozel and G. E. Stillman (INSPEC, London, 1996), p. 693.
[2] M. R. Melloch, N. Otsuka, J. M. Woodall, A. C. Warren, and J. L. Freeouf, Appl. Phys. Lett. **57**, 1531 (1990).
[3] P. A. Loukakos, C. Kalpouzos, I. E. Perakis, Z. Hatzopoulos, M. Logaki, and C. Fotakis, Appl. Phys. Lett. **79**, 2883 (2001).
[4] H. Ruda and A. Shik, Phys. Rev. B **63**, 085203 (2001).
[5] S. D. Benjamin, H. S. Loka, A. Othonos, and P. W. E. Smith, Appl. Phys. Lett. **68**, 2544 (1996).
[6] P. Grenier and J. F. Whitaker, Appl. Phys. Lett. **70**, 1998 (1997).
[7] T. S. Sosnowski, T. B. Norris, H. H. Wang, P. Grenier, J. F. Whitaker, and C. Y. Sung, Appl. Phys. Lett. **70**, 3245 (1997).
[8] M. Stellmatcher, J. P. Schnell, D. Adam, and J. Nagle, Appl. Phys. Lett. **74**, 1239 (1999).
[9] S. Gupta, M. Y. Frankel, J. A. Valdmanis, J. F. Whitaker, G. A. Mourou, F. W. Smith, and A. R. Calawa, Appl. Phys. Lett. **59**, 3276 (1991).
[10] U. Siegner, R. Fluck, G. Zhang, and U. Keller, Appl. Phys. Lett. **69**, 2566 (1996).
[11] M. Haiml, U. Siegner, F. Morier-Genoud, U. Keller, M. Luysberg, P. Specht, and E. R. Weber, Appl. Phys. Lett. **74**, 1269 (1999).
[12] M. Haiml, U. Siegner, F. Morier-Genoud, U. Keller, M. Luysberg, R. C. Lutz, P. Specht, and E. R. Weber, Appl. Phys. Lett. **74**, 3134 (1999).
[13] T. Okuno, Y. Masumoto, M. Ito, and H. Okamoto, Appl. Phys. Lett. **77**, 58 (2000).
[14] M. Stellmacher, J. Nagle, J. F. Lampin, P. Santoro, J. Vaneecioo, and A. Alexandro, J. Appl. Phys. **88**, 6026 (2000).
[15] A. J. Lochtefeld, M. R. Melloch, J. C. P. Chang, and E. S. Harmon, Appl. Phys. Lett. **69**, 1465 (1996).
[16] R. Yano, Y. Hirayama, S. Miyashita, H. Sasabu, N. Uesugi, and S. Uehara, Phys. Lett. A **289**, 93 (2001).
[17] D. S. Chemla and D. A. B. Miller, J. Opt. Soc. Am. B **2**, 1155 (1985).
[18] A. Suda and N. Otsuka, Surf. Sci. **458**, 162 (2000).
[19] M. Luysberg, H. Sohn, A. Prasad, P. Specht, Z. Liliental-Weber, E. R. Weber, J. Gebauer, and R. Krause-Rehberg, J. Appl. Phys. **83**, 561 (1998).
[20] W. Shockley and W. T. Read, Phys. Rev. **87**, 835 (1952).
[21] R. N. Hall, Phys. Rev. **87**, 387 (1952).
[22] S. Fukushima, T. Obata, and N. Otsuka, J. Appl. Phys. **89**, 380 (2001).
[23] S. A. Merritt and M. Dagenais, J. Electrochem. Soc. **140**, L138 (1993).
[24] D. A. B. Miller, D. S. Chemla, D. J. Eilenberger, P. W. Smith, A. C. Gossard, and W. Wiegmann, Appl. Phys. Lett. **42**, 925 (1983).
[25] S. Schmitt-Rink, D. S. Chemla, and D. A. B. Miller, Phys. Rev. B **32**, 6601 (1985).
[26] D. S. Chemla, D. A. B. Miller, P. W. Smith, A. C. Gossard, and W. Wiegmann, IEEE J. Quantum Electron. **QE-20**, 265 (1984).
[27] P. Silverberg, P. Omling, and L. Samuelson, Appl. Phys. Lett. **52**, 1689 (1988).
[28] W. H. Knox, C. Hirlimann, D. A. B. Miller, J. Shah, D. S. Chemla, and C. V. Shank, Phys. Rev. Lett. **56**, 1191 (1986).
[29] J. Krüger, Y. C. Shih, L. Xiao, C. L. Wang, J. D. Morse, M. Rogalla, K. Runge, and E. R. Weber, Proc. IEEE **SIMC-9**, 345 (1996).